—Full Paper—

Signal changes in standing magnetic resonance imaging of osseous injury at the origin of the suspensory ligament in four Thoroughbred racehorses under tiludronic acid treatment

Fumiaki MIZOBE[1]*, Motoi NOMURA[1], Tomohiro KATO[1], Yasuo NAMBO[2] and Kazutaka YAMADA[3]

[1]Racehorse Hospital, Ritto Training Center, Japan Racing Association, Shiga 520-3085, Japan
[2]Department of Clinical Veterinary Science, Obihiro University of Agriculture and Veterinary Medicine, Hokkaido 080-8555, Japan
[3]Laboratory of Veterinary Radiology, School of Veterinary Medicine, Azabu University, Kanagawa 252–5201, Japan

Problems associated with the proximal metacarpal region, such as an osseous injury associated with tearing of Sharpey's fibers or an avulsion fracture of the origin of the suspensory ligament (OISL), are important causes of lameness in racehorses. In the present study, four Thoroughbred racehorses (age range, 2–4 years) were diagnosed as having forelimb OISL and assessed over time by using standing magnetic resonance imaging (sMRI). At the first sMRI examination, all horses had 3 characteristic findings, including low signal intensity within the trabecular bone of the third metacarpus on T1-weighted images, intermediate-to-high signal intensity surrounded by a hypointense rim on T2*-weighted images, and high signal intensity on fat-suppressed images. Following the sMRI examination, all horses received 50 mg of tiludronic acid by intravenous regional limb perfusion once weekly for 3 weeks. Attenuation of the high signal intensity on T2*-weighted and fat-suppressed images was observed on follow-up sMRI in 3 horses. Following rest and rehabilitation, these 3 horses successfully returned to racing. In contrast, the other horse that did not show attenuation of the high signal intensity failed to return to racing. To our knowledge, this is the first report of OISL in Thoroughbred racehorses assessed over time by sMRI under tiludronic acid treatment. Our findings support the use of sMRI for examining lameness originating from the proximal metacarpal region to refine the timing of returning to exercise based on follow-up examinations during the recuperation period.
Key words: *magnetic resonance imaging, osseous injury, proximal metacarpus, racehorse, tiludronic acid*

The proximal metacarpal region is a common site of origin of lameness in racehorses [7]. Lameness can be related to an osseous injury associated with tearing of the Sharpey's fibers or an avulsion fracture of the origin of the suspensory ligament (OISL) [9]. As an etiology of OISL, hyperextension of the carpus has been proposed, which could cause stress and compression at a rate that exceeds the bone's ability to adapt [1]. An avulsion fracture is defined as a fracture at the stage when the palmar surface of the proximal third metacarpal bone (MC3) is torn away. Once progression to an avulsion fracture occurs, several months of rest and rehabilitation are required [3]. During the period of rest and rehabilitation, it is recommended that the progress of healing be followed by diagnostic imaging to formulate a prognosis and adapt the rehabilitation program.

Imaging diagnosis of an OISL generally involves radiography and ultrasonography. Changes in radiopacity at the origin of suspensory ligament (SL) can be detected in chronically lame horses or horses with a complete avulsion fracture [9]. However, these changes are not always

evident in acute or less severe cases [8]. Evaluation of ultrasonographic changes of the proximal metacarpal region has limitations and is sometimes challenging because of the limited acoustic accessibility [18]. The procedure generally includes scanning the SL and palmar surface of the MC3 [9]. It is possible to identify these abnormalities on sagittal scans, but usually obliquity can distort the shape of the SL, which makes it difficult to correctly interpret the image [18].

Magnetic resonance imaging (MRI) allows superior visualization of soft tissues and osseous anatomy, including fluid accumulation in and around ligaments and bones, such as hemorrhage, inflammation, edema, or joint fluid [26]. The use of MRI for investigation of suspected proximal metacarpal lameness was first described by using conventional MRI under general anesthesia [25]. Development of equine-dedicated standing MRI (sMRI), which allows scanning under sedation, has further expanded its application to the proximal metacarpal region [15]. Additionally, MRI has been suggested to have the potential to detect underlying pathologies even in the absence of conclusive radiographic and ultrasonographic findings in and around lesions [3].

Tiludronic acid (TA) is a non-nitrogenous bisphosphonate that inhibits osteoclast-mediated bone resorption and suppresses inflammation by decreasing nitric oxide and cytokines [12]. TA was originally used to treat conditions associated with increased bone turnover, such as navicular disease [6]. Recently, there has been a growing demand for use of TA to treat various musculoskeletal disorders, such as distal tarsal osteoarthritis, thoracolumbar osteoarthritis, and dorsal metacarpal disease, in equine medicine [5, 19]. However, signal changes in sMRI before and after TA have not been fully investigated.

To date, limited information has been available in the literature regarding sMRI findings of OISL in Thoroughbred racehorses undergoing full training [15]. Further, follow-up sMRI is expected to allow assessment of healing along with possible modification of rehabilitation, but the significance of the signal changes over time is not completely understood. The aim of the present study was to document imaging characteristics of 4 Thoroughbred racehorses with OISL under TA treatment repeatedly assessed by sMRI and to relate these findings to the results of other imaging modalities.

Materials and Methods

Case selection

All horses that were presented to the Racehorse Hospital, Ritto Training Center, between 2015 and 2016 for lameness evaluation and diagnosed as having OISL by sMRI were included in this study.
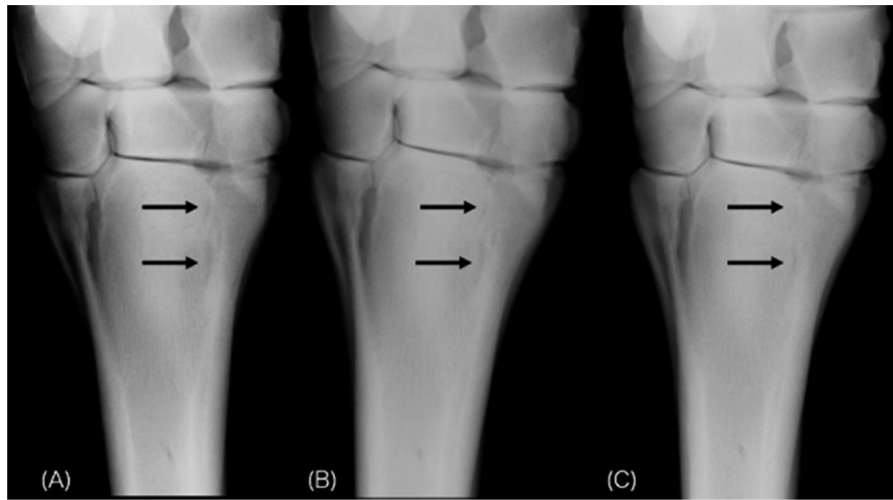
Radiography and ultrasonography

Radiographs were taken by using a computed digital radiography system (FCR Speedia CS, Fujifilm, Tokyo, Japan). In all cases, radiographic projections included standing dorsopalmar, dorsolateral palmaromedial 45° oblique, and dorsomedial palmarolateral 45° oblique views of the proximal metacarpal region. Ultrasonographic evaluation of the proximal palmar metacarpal region was performed by using an ultrasound system (HI VISION Avius, Hitachi, Tokyo, Japan) with a 6–14 MHz linear probe.
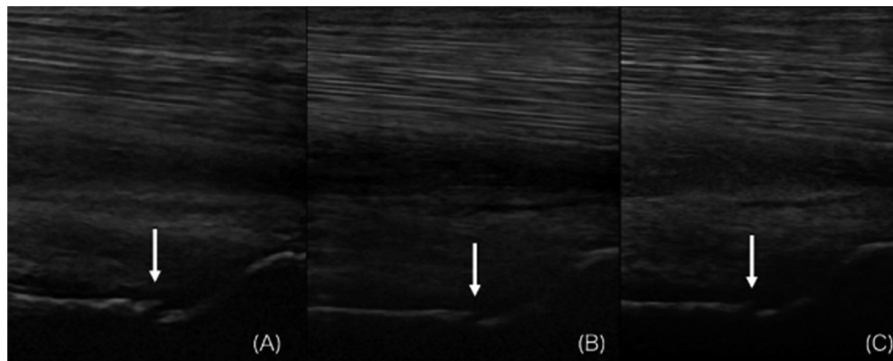
Standing MRI

A 0.27-Tesla equine-dedicated MRI system (Equine Limb Scanner; Hallmarq Veterinary Imaging, Ltd., Guildford, U.K.) was used to obtain MRI images of the proximal metacarpal region. T1-weighted gradient echo (GRE) (echo time [TE], 8 msec; repetition time [TR], 52 msec; flip angle, 50°), T2*-weighted GRE (TE,13 msec; TR, 68 msec; flip angle, 28°) and short tau inversion recovery (STIR) fast spin echo (FSE) (TE, 22 msec; TR, 2,536 msec; inversion time [TI], 120 msec), which uses a fat suppression technique, were acquired in the transverse and sagittal planes. All horses were sedated while undergoing sMRI. Medetomidine (Domitor, Zenoaq Nippon Zenyaku Kogyo Co., Ltd., Fukushima, Japan) was administered at an initial dose of 5 μg/kg prior to the onset of positioning within the magnet. Thereafter, small doses of medetomidine (0.2 μg/kg) were administered periodically to maintain sufficient tranquilization for the scan. MRI images were acquired and reviewed by clinicians (F. M., M. N., T. K.) experienced in the interpretation of sMRI images of Thoroughbred racehorses by using the OsiriX Digital Imaging and Communications in Medicine viewer (version 3.9.2; OsiriX Project, Geneva, Switzerland). Osseous lesions identified by sMRI in the proximal metacarpus were graded on the basis of the presence of low signal intensity on T1-weighted images and the size of high signal intensity on T2*-weighted and fat-suppressed images, as defined according to the following criteria: profound, intermediate-to-high signal intensity surrounded by a hypointense rim on T2*-weighted images and markedly high signal intensity on fat-suppressed images; severe, intermediate-to-high signal intensity surrounded by a hypointense rim on T2*-weighted images and high signal intensity on fat-suppressed images; moderate, low signal intensity on T1-weighted images and high signal intensity on fat-suppressed images; mild, low signal intensity on T1-weighted images.

TA administration

All horses received intravenous regional limb perfusion (RLP) of TA (Tildren, CEVA, Ltd., Libourne, France) once weekly for 3 consecutive weeks. Briefly, the cephalic vein

Fig. 1. Dorsopalmar radiographic images of the right metacarpus of case 1 on day 2 (A), day 53 (B), and day 87 (C). Linear radiolucent lesions are evident at the proximal medial surface of the third metacarpus throughout the period (arrows).

Fig. 2. Sagittal ultrasonographic images of case 1, acquired in a standing palmar position over the proximal right metacarpal region on day 3 (A), day 53 (B), and day 87 (C). The proximal is at right, and the distal direction is at left. A hyperechogenic fragment is identifiable on the palmar cortex of the third metacarpal bone (A; arrow), and the surface irregularity remain visible throughout the period (B, C; arrow).
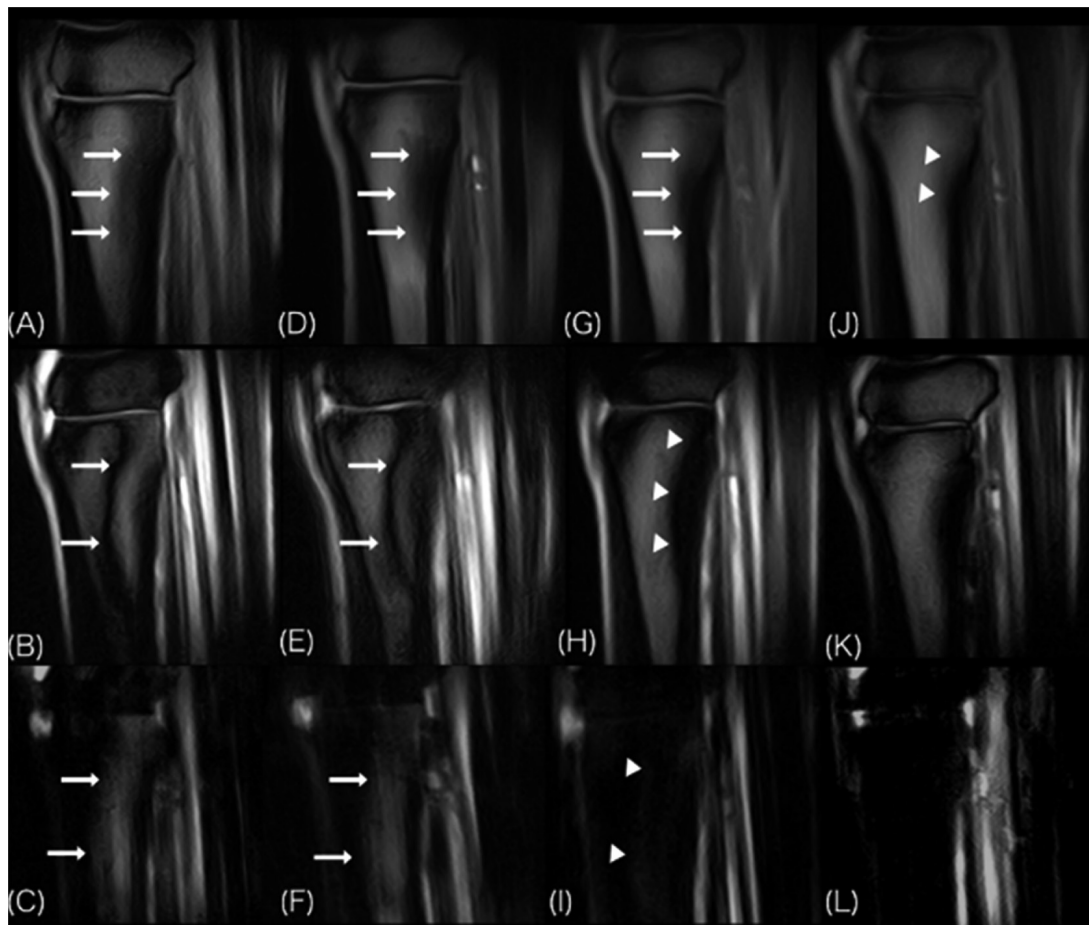
in the affected limb was isolated by using a tourniquet. Thereafter, 50 mg of TA diluted in 40 m*l* of saline was injected through a 22-gauge butterfly catheter placed in the cephalic vein. The tourniquet was removed after 30 min. The dose and route of administration adopted in the present study were approved beforehand by the Japan Racing Association Committee of Safe and Ethical Use of Medication. Additionally, the TA administration was performed under the consent of the owners of each case.

Results

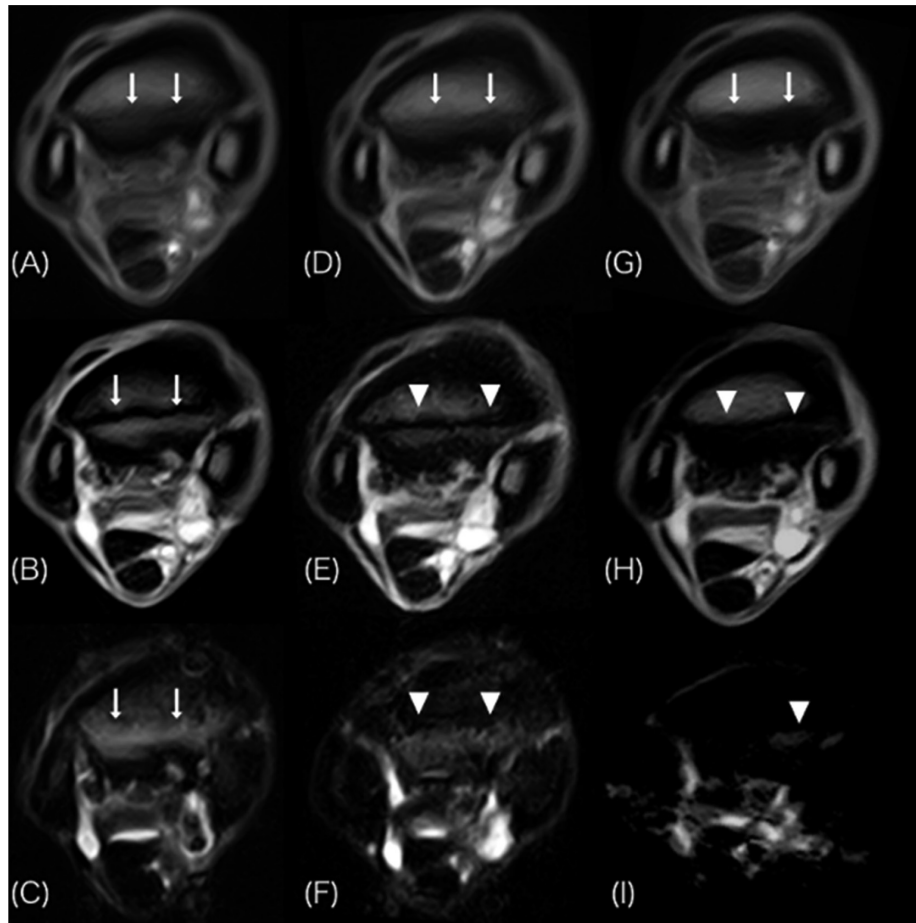*Case 1*

A 2-year-old Thoroughbred colt exhibited acute-onset right foreleg lameness following exercise. There was swelling, heat, and pain in the palmar aspect of the proximal metacarpus. On day 2, radiography revealed linear radiolucent lesions at the palmaromedial surface of the proximal MC3 (Fig. 1A). In addition, a hyperechogenic fragment was identified on the palmar cortex of the MC3 by ultrasonography (Fig. 2A). To obtain additional information for diagnosis, sMRI was performed on day 3. It revealed low signal intensity in the trabecular bone of the MC3 on T1-weighted images, whereas the area showed intermediate-to-high signal intensity surrounded by a hypointense rim on T2*-weighted images and markedly high signal intensity on fat-suppressed images (Fig. 3A–C). Thereafter, the colt received a series of TA treatments on days 3, 10, and 17. On

Fig. 3. Sagittal T1-weighted, T2*-weighted, and fat-suppressed images on day 3 (A, B, C), day 24 (D, E, F), day 53 (G, H, I), and day 87 (J, K, L), respectively (all days), from case 1, acquired at the level of the proximal half of the right metacarpus. The proximal and dorsal directions are at the top and left, respectively. An area of low signal intensity within the trabecular bone of the third metacarpus is visible on a T1-weighted image from day 3 (A; arrows). The area has intermediate-to-high signal intensity surrounded by a hypointense rim on a T2*-weighted image (B; arrows) with a corresponding markedly high signal intensity on a fat-suppressed image (C; arrows). The high signal intensity is attenuated on a T2*-weighted image from day 53 (H; arrowheads). The area of high signal intensity is significantly decreased on a fat-suppressed image (I; arrowheads). The area of decreased signal intensity is slightly decreased on a T1-weighted image from day 87 (J; arrowheads). The high signal intensity is no longer observed on a T2*-weighted image (K) and fat-suppressed image (L).

day 24, the colt underwent a second sMRI, which showed a decreased area of high signal intensity on T2*-weighted and fat-suppressed images (Fig. 3E and 3F). By day 24, the lameness was no longer apparent during walking. The swelling, heat, and pain in the palmar aspect of the proximal metacarpus were reduced. On the other hand, there was little change on radiographic or ultrasonographic images. A third sMRI was performed on day 53, and it showed attenuation of the high signal intensity on T2*-weighted images and a significant decrease in the area of high signal intensity on fat-suppressed images (Fig. 3H and 3I). In contrast, linear radiolucent lesions remained visible on radiographic images

(Fig. 1B), and a surface irregularity of the palmar cortex of MC3 was identified on ultrasonographic images (Fig. 2B). The swelling and heat in the palmar aspect of the proximal metacarpus were completely resolved, whereas slight pain was still elicited by palpation. A fourth sMRI was performed on day 87, which confirmed attenuation of the high signal intensity on fat-suppressed images (Fig. 3L). The linear radiolucent lesions and the surface irregularity were identifiable on radiographic images (Fig. 1C) and ultrasonographic images (Fig. 2C), respectively. The lameness was no longer recognizable during trotting, and there were no abnormalities on palpation.

Fig. 4. Transverse T1-weighted, T2*-weighted, and fat-suppressed images on day 1 (A, B, C), day 23 (D, E, F), and day 85 (G, H, I), respectively (all days), from case 2, acquired at 2 cm distal to the right carpometacarpal joint. Dorsal is to the top and lateral is to the left. There is low signal intensity in the cancellous bone of the third metacarpus in a T1-weighted sequence from day 1 (A; arrows). The area has intermediate-to-high signal intensity surrounded by a hypointense rim on a T2*-weighted image (B; arrows) and markedly high signal intensity on a fat-suppressed image (C; arrows). There is a decrease in the area of high signal intensity on a T2*-weighted (E; arrowheads) and fat-suppressed images from day 23 (F; arrowheads). The area of low signal intensity remains visible on a T1-weighted image from day 85 (G; arrows), whereas the area of high signal intensity is attenuated on a T2*-weighted image (H; arrowheads) and significantly decreased on a fat-suppressed image (I; arrowhead).

The colt was box rested during the first 24 days and then started walking exercises 30 min/day until the third sMRI examination. Thereafter, the duration of the walking exercise was extended to 60 min/day. Following the fourth sMRI examination, the colt resumed ridden exercise, and it commenced full training (herein, defined as fast canter work) on day 184. Other than TA, no medication was given to the colt during the rehabilitation period. Eventually, the colt returned to racing on day 242. The colt ran 2 more races afterwards without reinjury.

Case 2

A 4-year-old Thoroughbred colt exhibited right foreleg lameness after exercise. The palmar aspect of the proximal metacarpus was swollen, and the colt showed a marked pain response by palpation. Radiography identified a focal semi-circular area of increased radiolucency at the proximal MC3 (Suppl. Fig. 2A). Ultrasonography did not yield any particular findings. Thereafter, sMRI was performed for further evaluation. It revealed low signal intensity in the trabecular bone of the MC3 on T1-weighted images, whereas the area showed intermediate-to-high signal intensity surrounded by a hypointense rim on T2*-weighted images and mark-

edly high signal intensity in fat-suppressed images (Fig. 4A–C). Following the sMRI examination, the colt received a series of TA treatments on days 2, 9, and 16. On day 23, a second sMRI identified decreased signal intensity in the area of high signal intensity on both T2*-weighted and fat-suppressed images (Fig. 4E and 4F). At this point, lameness was not recognizable during walking. The swelling over the palmar aspect of the proximal metacarpus was reduced, but there was still pain around the area. In radiography, the focal semicircular area of increased radiolucency was still evident (Suppl. Fig. 2B). A third sMRI was performed on day 85, and it showed attenuation of the high signal intensity on T2*-weighted images and a significant decrease in the area of high signal intensity on fat-suppressed images (Fig. 4H and 4I). By day 85, the lameness and pain had subsided, but mildly increased radiolucency remained visible on radiographic images (Suppl. Fig. 2C). There were no abnormalities in the ultrasonographic images.

The colt was prescribed 23 days of boxed rest followed by a gradual return to walking exercise. After the third sMRI, the colt resumed ridden exercise, and it returned to full training on day 191. No medication was given to the colt during the rehabilitation period. The colt returned to racing on day 228 and won its 7th race after the injury. The colt did not show any signs of lameness for >1 year.

Case 3

A 3-year-old Thoroughbred colt exhibited acute-onset left foreleg lameness following a race on a flat turf course. On admission, there was swelling over the palmar aspect of the proximal metacarpus. Radiography was performed to determine the cause of this symptom, but it did not yield any particular findings. Perineural anesthesia of the palmar nerves and palmar metacarpal nerves by using 2% mepivacaine (Mepivacaine, AstraZeneca K.K., Osaka, Japan) together with infiltration of the local anesthetics just below the accessory carpal bone eliminated the lameness. Therefore, sMRI was performed to examine the proximal metacarpal region on day 6. A focal area of low signal intensity within the trabecular bone of the MC3 on T1-weighted images was observed (Fig. 5A). In T2*-weighted sequences, the area was imaged as a focal intermediate-to-high signal intensity lesion surrounded by a hypointense rim, whereas the area had diffusely high signal intensity on fat-suppressed images (Fig. 5B and 5C). On the basis of the findings, the colt received a series of TA treatments on days 6, 13, and 20. On day 20, a second sMRI detected attenuation of the high signal intensity on T2*-weighted images, whereas the high signal intensity remained visible on fat-suppressed images (Fig. 5E and 5F). There were no abnormalities on radiography. The swelling in the palmar aspect of the proximal metacarpus was substantially reduced at this point.

The colt was box rested until the second sMRI and then started walking exercise. The colt resumed ridden exercise on day 90, and it resumed full training on day 181. By day 181, no medication was given to the colt other than TA. Unfortunately, the colt suffered from a left carpal fracture on day 280 and eventually returned to racing on day 441. Although the colt did not show symptoms of reinjury, the owner was unwilling to race the colt any longer considering its race result and chose to retire the colt from racing.

Case 4

A 3-year-old Thoroughbred filly was referred to the hospital with right foreleg lameness after exercise and swelling over the palmar aspect of the proximal metacarpus. On day 2, radiography identified increased radiolucency of the proximal MC3 (Suppl. Fig. 3A). sMRI images taken on the same day showed intermediate-to-high intraosseous signal intensity surrounded by a hypointense rim on T2*-weighted images and marked hyperintensity on fat-suppressed images with corresponding T1-weighted hypointensity (Fig. 6A–C). Despite a series of TA treatments on days 2, 9, and 16, the increased radiolucency (Suppl. Fig. 3B) and high signal intensity on T2*-weighted and fat-suppressed images (Fig. 6E and 6F) remained unchanged until day 16. Palpation over the palmar aspect of the proximal metacarpus revealed slight reduction of the swollen area.
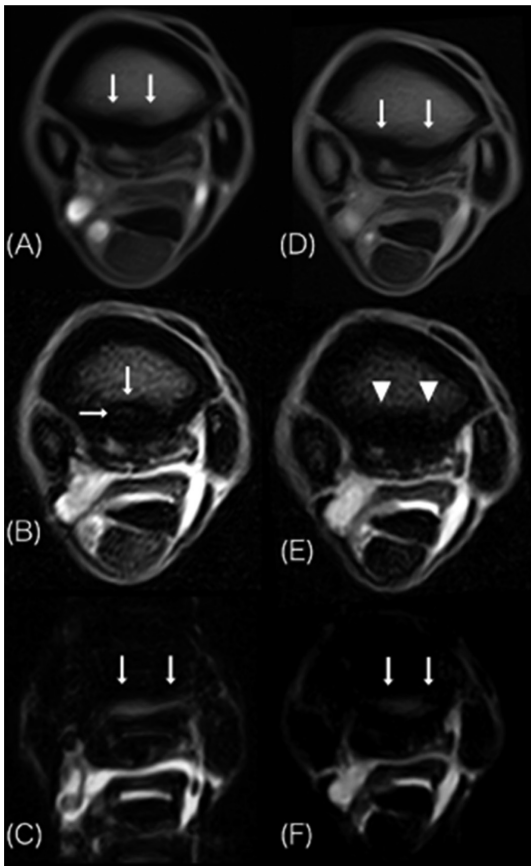
Following the sMRI examination, the filly retired from racing due to the financial reasons of the owner.

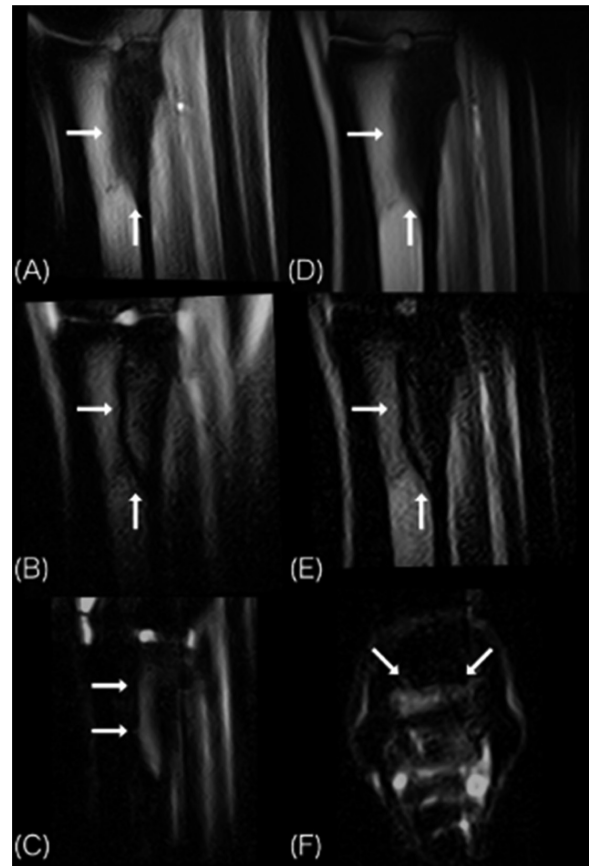*Summary of the results of cases 1–4*

The sMRI findings of each case are summarized in Table 1 together with the radiographic and ultrasonographic findings for comparison. Table 2 shows the sMRI findings, degrees of lameness, findings by palpation, and exercise intensities of each case.

Discussion

The proximal metacarpal region is a common site for performance-limiting lameness in Thoroughbred racehorses [7]. Advances in imaging modalities, such as MRI and nuclear scintigraphy, have increased attention regarding lameness arising from the region in clinical practice, and several types of injuries are now widely recognized [1]. Recently, in place of conventional MRI, sMRI has been used with increased frequency in the investigation of proximal metacarpal region pain, and it has been shown to be useful for detection of lesions that cannot be diagnosed by other imaging modalities [3]. In the forelimbs, insertional desmopathies of the SL, inferior check ligament desmitis, and OISL should be considered in the differential

Fig. 5. Transverse T1-weighted, T2*-weighted, and fat-suppressed images on day 6 (A, B, C) and day 20 (D, E, F), respectively (both days), from case 3, acquired at 2 cm distal to the left carpometacarpal joint. The dorsal and medial directions are at the top and left, respectively. A focal area of low signal intensity within the cancellous bone of the third metacarpus is visible on a T1-weighted image from day 6 (A; arrows). The area is imaged as a focal intermediate-to-high signal intense lesion surrounded by a hypointense rim on a T2*-weighted image (B; arrows), whereas the area shows high signal intensity on a fat-suppressed image (C; arrows). The area of decreased signal intensity is visible on a T1-weighted image from day 20 (D; arrows). The area of high signal intensity is attenuated on a T2*-weighted image (E; arrowheads), whereas the high signal intensity remains visible on a fat-suppressed image (F; arrows).

Fig. 6. Sagittal T1-weighted, T2*-weighted, and fat-suppressed images on day 2 (A, B, C) and day 16 (D, E), respectively (both days), from case 4, acquired at the level of the proximal half of the right metacarpus. The proximal and dorsal directions are at the top and left, respectively. An area of low signal intensity within the trabecular bone of the third metacarpus is visible on a T1-weighted image from day 2 (A; arrows), whereas the area has intermediate-to-high signal intensity surrounded by a hypointense rim on a T2*-weighted image (B; arrows) and markedly high signal intensity on a fat-suppressed image (C; arrows). The high signal intensity is still evident on a T2*-weighted image from day 16 (E; arrows) and also remains visible on a transverse fat-suppressed image (F; arrows).

diagnosis [1]. All cases in the present study were diagnosed as having an OISL, which indicated the usefulness of sMRI for reaching clinical diagnosis of lameness originating from the proximal metacarpal region.

In this study, all cases were initially examined by radiography. The primary importance of radiography is to rule out fracture and to examine bone changes, such as bone resorption and new bone formation. In cases 2 and 4, radiography revealed a focal radiolucent area at the proximal MC3, which probably indicated the presence of

an avulsion fracture. Relatively large linear radiolucent lesions were detected in case 1, which suggested that the fracture may have been more appropriately classified as an incomplete fracture. In contrast, changes in radiolucency were not observed by radiography despite the presence of fluid accumulation on sMRI images in case 3. From this, it was inferred that lack of radiographic findings does not necessarily preclude problems in the proximal metacarpal region. It is possible that case 3 was imaged prior to the overt fracture taking place, which would suggest the poten-

Table 1. Standing magnetic resonance imaging (sMRI), radiographic, and ultrasonographic findings of cases 1–4

Case	Day	sMRI findings in the proximal metacarpus	Radiographic findings in the proximal metacarpus	Ultrasonographic findings in the proximal metacarpus
1	3	Profound	Increase in radiolucency (day 2)	Hyperechogenic fragmentation
	24	Severe	Increase in radiolucency	Hyperechogenic fragmentation
	53	Moderate	Increase in radiolucency	Surface irregularity
	87	Mild	Increase in radiolucency	Surface irregularity
2	1	Profound	Increase in radiolucency	NAD
	23	Severe	Increase in radiolucency	NAD
	85	Moderate	Mild increase in radiolucency	NAD
3	6	Severe	NAD (day 5)	-
	20	Moderate	NAD	-
4	2	Profound	Increase in radiolucency	-
	16	Profound	Increase in radiolucency	-

Osseous lesions identified by sMRI in the proximal metacarpus are graded as mild, moderate, severe, or profound on the basis of the presence of low signal intensity on T1-weighted images and the size of high signal intensity on T2*-weighted and fat-suppressed images. NAD=no significant abnormalities detected.

Table 2. Standing magnetic resonance imaging (sMRI) findings, degree of lameness, finding by palpation, and exercise intensity of cases 1–4

Case	Day	sMRI findings	Degrees of lameness	Findings by palpation	Exercise intensities
1	3	Profound	Obvious at a walk	Marked swelling and pain	Boxed rest
	24	Severe	Obvious at a trot	Swelling and pain	Walking (30 min/day)
	53	Moderate	NAD	Slight pain	Walking (60 min/day)
	87	Mild	NAD	NAD	Ridden exercise
	184	-	-	-	Full training
	242	-	-	-	Return to racing
		Remarks: Running a total of 3 races without reinjury			
2	1	Profound	Obvious at a walk	Swelling and marked pain	Boxed rest
	23	Severe	Obvious at a trot	Slight swelling and pain	Walking
	85	Moderate	NAD	NAD	Ridden exercise
	191	-	-	-	Full training
	228	-	-	-	Return to racing
		Remarks: Running a total of 7 races without reinjury			
3	6	Severe	Obvious at a trot	Swelling	Boxed rest
	20	Moderate	NAD	Slight swelling	Walking
	90	-	NAD	NAD	Ridden exercise
	181	-	-	-	Full training
	280	-	Obvious at a walk	Carpal fracture	Boxed rest
	441	-	-	-	Return to racing
		Remarks: Running 1 race without reinjury, but subsequently retired due to other reasons			
4	2	Profound	Obvious at a walk	Marked swelling	Boxed rest
	16	Profound	Obvious at a walk	Swelling	Boxed rest
		Remarks: Retired due to financial reasons			

Osseous lesions identified by sMRI in the proximal metacarpus are graded as mild, moderate, severe, or profound on the basis of the presence of low signal intensity on T1-weighted images and the size of high signal intensity on T2*-weighted and fat-suppressed images. NAD=no significant abnormalities detected.

tial usefulness of sMRI for early detection of prodromal fractures. In histology, the origin of the SL is characterized by dense collagenous connective tissue [2, 16]. Healing of an injury at the origin of the SL is known to involve formation of enthesophytes, but in the early stages of new bone formation, radiopacity is known to have a vague radiographic appearance, which then progresses to a more structured pattern over time [4]. The follow-up sMRIs of the present cases identified a decrease in the area of osseous injury before radiographic improvement became evident,

which indicated that sMRI could be superior to radiography in evaluating an OISL throughout the healing process.

In the present study, 2 cases underwent ultrasonography. In case 1, an avulsion fragment was identifiable 2 cm distal to the carpometacarpal joint on day 2. Although there was improvement of clinical symptoms and a decrease in the area of osseous injury detected by sMRI, the irregularity of the palmar surface of the proximal MC3 remained visible on follow-up ultrasonography. Additionally, ultrasonography failed to detect abnormalities in case 2. It has been reported that interpretation of ultrasonographic images of the proximal metacarpal region could be somewhat subjective and that the technique is prone to a variety of artifacts [8, 24]. The results of the current study indicated that ultrasonography could be inconclusive for identifying an OISL, and surface irregularity of the MC3 might not be a good indicator for monitoring the healing process. Occasionally, an OISL may involve insertional desmopathy of the SL, and therefore evaluation of structural changes of the SL would be recommended [1]. In ultrasonographic measurement of the shape of the proximal SL, it has been postulated that intraoperator variability would be unavoidable [24]. The diagnostic accuracy and utility of MRI compared with those of ultrasonography regarding proximal SL assessment remains a point of discussion [22]. In the present study, the SL appeared as areas of mixed signal intensity on all sMRI sequences adopted. Because the SL is a modified ligament that contains sparse muscle fibers that contain nerves, vessels, and adipose tissues [23], it is conceivable that the proximal SL is imaged as a non-homogenous structure by sMRI. In fact, high signal intensity was also observed within the SL on T1-weighted GRE images from a sound horse in the current study. Therefore, it was presumed that the clinical significance of a variety of sMRI signal intensities within the SL should be interpreted with caution.

In the present study, the following sequences were used in the sMRI examination: T1-weighted GRE, T2*-weighted GRE, and STIR FSE. All cases exhibited signal changes within the trabecular bone, which were characterized by decreased signal intensity on T1-weighted images, intermediate-to-high signal intensity surrounded by a hypointense rim on T2*-weighted images, and increased signal intensity on fat-suppressed images. The signal changes were assumed to be related to the transient increase in bone marrow water content with hyperemia or replacement of bone marrow fat by material containing H+ ions, such as water [10, 14]. In T2*-weighted sequences, the area of intermediate-to-high signal intensity was surrounded by a hypointense rim, presumably because of a phase effect cancellation [21]. Phase effect cancellation is seen when an equal amount of fat and water is present in areas of trabecular bone, which makes signals from both fat and water cancel each other and

results in an area of zero signal intensity. This effect was suggested to be useful to highlight fluid-based pathology in the bone. For example, diffusely decreased signal intensity within the trabecular bone on T1-weighted images, which was observed in the present study, could indicate bone sclerosis, in the absence of phase effect cancellation on T2*-weighted GRE images or high signal intensity on fat-suppressed images [17].

In cases 1, 2, and 3, high intraosseous signal intensity remained visible on fat-suppressed images at the point where the signal abnormality in T2*-weighted sequences resolved. The STIR FSE sequence, which uses a fat suppression technique, has been reported to outweigh the T2*-weighted sequence for evaluating fat-based tissues, such as the trabecular bone [13]. This is theoretically because the normal high signal of fat in the trabecular bone is suppressed in the fat suppression sequence, which allows detection of bone lesions that would be inconspicuous in other sequences. On the other hand, one practical advantage of the T2*-weighted sequence over the STIR FSE sequence would be a shorter acquisition time. A longer acquisition time increases the risk of motion artifacts during sMRI because the images are obtained under standing sedation. In evaluating the presence of intraosseous fluid in anxious or difficult horses, the T2*-weighted sequence should be particularly useful in situations in which excess motion could result in poor quality STIR FSE images. In the present study, 3 horses that resumed exercise in accordance with healing of their osseous injuries successfully returned to racing. These horses showed characteristic signal changes, which were attenuation of high signal intensity in T2*-weighted sequences together with a significant decrease in areas of high signal intensity on fat-suppressed images. The results of the current study suggest that these characteristic signal changes should be interpreted as indicating the proper timing for horses with OISL to commence ridden exercise. Unfortunately, the other horse that did not show attenuation of the high signal intensity retired from racing immediately after the second sMRI due to financial reasons of the owner. Therefore, the period it might have taken until the signal attenuation remained unclear for this horse.

The degrees of clinical symptoms in the present cases corresponded well with the cases of OISL described in a previous report [3]. Previous studies have suggested that the mean resting period required for OISL would be 3–6 months [1]. Anti-inflammatory medications and leg cooling would be recommended to reduce swelling in the acute stage. For early recovery and prevention of reinjury, injection of stem cells or platelet-rich plasma has become a common treatment option for injuries that involve significant core lesions within the SL [1]. In the current study, such core lesions were not detected. TA has reportedly been efficacious in

treatment of conditions associated with bone inflammation [6]. On the other hand, no literature is presently available in which the usefulness of TA in OISL cases was evaluated, despite its growing use in equine medicine. The dose and route of administration of TA in the present study were determined on the basis of a previous report [5]. The potential benefits of the use of TA via RLP would include reduced cost and occurrence of side effects, such as colic, relative to those of systemic administration. Meanwhile, repeated administration of TA via RLP may still require a long-term follow-up investigation of the effects on synovial cells [19]. It is conceivable that the concentration of TA in synovial fluid can be harmfully high after RLP, although differences in synovial inflammation between TA-administered and saline-administered limbs were not identified in a previous study [11]. Vanel *et al.* reported 34 horses with deep digital flexor tendinopathy, 15 of which were treated with systemic TA, and follow-up sMRI images were obtained for these horses [20]. However, the study mainly focused on the clinical outcome, and there was limited observation of changes in the imaging characteristics associated with TA. To the best of our knowledge, this is the first report of OISL in Thoroughbred racehorses assessed over time by sMRI under TA treatment. All but 1 horse in the present study successfully returned to racing following rest and rehabilitation, in which the exercise intensity was controlled and gradually increased over time with respect to the healing of the osseous injury detected by sMRI. Our results emphasize the importance of follow-up sMRI to obtain prognostic information based on the evolution of lesion signals under TA treatment. Assessment of the entire osseous injury could be an important landmark for image interpretation, and accordingly, T2*-weighted and fat-suppressed sequences would offer reliable information to refine rehabilitation programs and prediction of clinical outcomes.

A limitation of the present study was the lack of placebo-administered cases. Therefore, whether the healing of the osseous injuries was accelerated by TA remained unclear. According to a previous study using 8 racehorses, follow-up sMRI images were obtainable in only 1 of the cases after 3 months, which detected attenuation of the high signal intensity on T2*-weighted and fat-suppressed images [15], but it has been reported that the case did not receive any medication during the rehabilitation period. In comparison, a similar level of signal attenuation was observed in case 1 on day 87, whereas the high signal intensity on fat-suppressed images remained visible in case 2 on day 85. Above all, further studies are warranted to clarify the clinical efficacy of TA for Thoroughbred racehorses with an osseous injury.

In conclusion, OISL should be considered in the differential diagnosis of Thoroughbred racehorses with swelling over the palmar aspect of the proximal metacarpus.

Compared with radiography and ultrasonography, sMRI is an excellent diagnostic modality for the diagnosis of OISL. The image quality yielded by this modality is suitable for detailed evaluation of an osseous injury and assessment of healing under TA treatment to refine the timing of return to exercise.

Acknowledgments

References

1. Bertone, A.L. 2011. Suspensory ligament desmitis. pp. 644–648. *In*: Adams and Stashak's Lameness in Horses, 6th ed. (Baxter, G.M. ed.), Blackwell Publishing, Ltd., West Sussex.

2. Bischofberger, A.S., Konar, M., Ohlerth, S., Geyer, H., Lang, J., Ueltschi, G., and Lischer, C.J. 2006. Magnetic resonance imaging, ultrasonography and histology of the suspensory ligament origin: a comparative study of normal anatomy of warmblood horses. *Equine Vet. J.* **38**: 508–516. [Medline] [CrossRef]

3. Brokken, M.T., Schneider, R.K., Sampson, S.N., Tucker, R.L., Gavin, P.R., and Ho, C.P. 2007. Magnetic resonance imaging features of proximal metacarpal and metatarsal injuries in the horse. *Vet. Radiol. Ultrasound* **48**: 507–517. [Medline] [CrossRef]

4. Butler, J. 2000. Clinical radiology of the horse. pp. 158–165. *In:* Clinical Radiology of the Horse, 2nd ed. (Butler, J.A., Colles, C.M., Dyson, S.J., Kold, S.E. and Poulos, P.W. eds.), Blackwell Science, Ltd., Oxford.

5. Carpenter, R.S. 2012. How to treat dorsal metacarpal disease with regional tiludronate and extracorporeal shock wave therapies in thoroughbred racehorses. Proceedings of the 58th annual convention of the American Association of Equine Practitioners **58**: 546–549.

6. Denoix, J.M., Thibaud, D., and Riccio, B. 2003. Tiludronate as a new therapeutic agent in the treatment of navicular disease: a double-blind placebo-controlled clinical trial. *Equine Vet. J.* **35**: 407–413. [Medline] [CrossRef]

7. Dyson, S. 1991. Proximal suspensory desmitis: clinical, ultrasonographic and radiographic features. *Equine Vet. J.* **23**: 25–31. [Medline] [CrossRef]

8. Dyson, S.J. 2003. Proximal metacarpal and metatarsal pain: a diagnostic challenge. *Equine Vet. Educ.* **15**: 134–138. [CrossRef]

9. Dyson, S.J., Arthur, R.M., Palmer, S.E., and Richardson, D. 1995. Suspensory ligament desmitis. *Vet. Clin. North Am. Equine Pract.* **11**: 177–215. [Medline] [CrossRef]

10. Gonzalez, L.M., Schramme, M.C., Robertson, I.D., Thrall, D.E., and Redding, R.W. 2010. MRI features of

metacarpo(tarso)phalangeal region lameness in 40 horses. *Vet. Radiol. Ultrasound* **51**: 404–414. [Medline] [CrossRef]

11. Hunter, B.G., Duesterdieck-Zellmer, K.F., and Larson, M.K. 2015. Tiludronate concentrations and cytologic findings in synovial fluid after intravenous regional limb perfusion with tiludronate in horses. *PeerJ* **3**: e889 [CrossRef]. [Medline]

12. Kamm, L., McIlwraith, W., and Kawcak, C. 2008. A review of the efficacy of Tiludronate in the horse. *J. Equine Vet. Sci.* **28**: 209–214. [CrossRef]

13. Murray, R., and Mair, T. 2005. Use of magnetic resonance imaging in lameness diagnosis in the horse. *In Practice* **27**: 138–146. [CrossRef]

14. Olive, J., Mair, T.S., and Charles, B. 2009. Use of standing low-field magnetic resonance imaging to diagnose middle phalanx bone marrow lesions in horses. *Equine Vet. Educ.* **21**: 116–123. [CrossRef]

15. Powell, S.E., Ramzan, P.H.L., Head, M.J., Shepherd, M.C., Baldwin, G.I., and Steven, W.N. 2010. Standing magnetic resonance imaging detection of bone marrow oedema-type signal pattern associated with subcarpal pain in 8 racehorses: a prospective study. *Equine Vet. J.* **42**: 10–17. [Medline] [CrossRef]

16. Schramme, M., Josson, A., and Linder, K. 2012. Characterization of the origin and body of the normal equine rear suspensory ligament using ultrasonography, magnetic resonance imaging, and histology. *Vet. Radiol. Ultrasound* **53**: 318–328. [Medline]

17. Sherlock, C.E., Mair, T.S., and Ter Braake, F. 2009. Osseous lesions in the metacarpo(tarso)phalangeal joint diagnosed using low-field magnetic resonance imaging in standing horses. *Vet. Radiol. Ultrasound* **50**: 13–20. [Medline] [CrossRef]

18. Smith, R.K.W., and Cauvin, E.R.J. 2014. Ultrasonography of the metacarpus and metatarsus. pp. 92–95. *In:* Atlas of Equine Ultrasonography. (Kidd, J.A., Lu, K.G. and Frazer, M.L. eds.), John Wiley & Sons, Ltd., West Sussex.

19. Soto, S.A., and Barbara, A.C. 2014. Bisphosphonates: pharmacology and clinical approach to their use in equine osteoarticular diseases. *J. Equine Vet. Sci.* **34**: 727–737. [CrossRef]

20. Vanel, M., Olive, J., Gold, S., Mitchell, R.D., and Walker, L. 2012. Clinical significance and prognosis of deep digital flexor tendinopathy assessed over time using MRI. *Vet. Radiol. Ultrasound* **53**: 621–627. [Medline] [CrossRef]

21. Werpy, N. 2009. Diagnosis of middle phalanx bone marrow lesions in horses using magnetic resonance imaging and identification of phase effect cancellation for proper image interpretation. *Equine Vet. Educ.* **21**: 125–130. [CrossRef]

22. Werpy, N.M., Denoix, J.M., McIlwraith, C.W., and Frisbie, D.D. 2013. Comparison between standard ultrasonography, angle contrast ultrasonography, and magnetic resonance imaging characteristics of the normal equine proximal suspensory ligament. *Vet. Radiol. Ultrasound* **54**: 536–547. [Medline] [CrossRef]

23. Wilson, D.A., Baker, G.J., Pijanowski, G.J., Boero, M.J., and Badertscher, R.R. 2nd. 1991. Composition and morphologic features of the interosseous muscle in Standardbreds and Thoroughbreds. *Am. J. Vet. Res.* **52**: 133–139. [Medline]

24. Zauscher, J.M., Estrada, R., Edinger, J., and Lischer, C.J. 2013. The proximal aspect of the suspensory ligament in the horse: how precise are ultrasonographic measurements? *Equine Vet. J.* **45**: 164–169. [Medline] [CrossRef]

25. Zubrod, C.J., Schneider, R.K., and Tucker, R.L. 2004. Use of magnetic resonance imaging identify suspensory desmitis and adhesions between exostoses of the second metacarpal bone and the suspensory ligament in four horses. *J. Am. Vet. Med. Assoc.* **224**: 1815–1820, 1789. [Medline] [CrossRef]

26. Zubrod, C.J., Schneider, R.K., Tucker, R.L., Gavin, P.R., Ragle, C.A., and Farnsworth, K.D. 2004. Use of magnetic resonance imaging for identifying subchondral bone damage in horses: 11 cases (1999−2003). *J. Am. Vet. Med. Assoc.* **224**: 411–418. [Medline] [CrossRef]